

Nanogap quantum dot photodetectors with high sensitivity and bandwidth

Michael C. Hegg,^{a)} Matthew P. Horning, Tom Baehr-Jones, Michael Hochberg, and Lih Y. Lin^{b)}

Department of Electrical Engineering, University of Washington, Seattle, Washington 98195-2500, USA

(Received 25 January 2010; accepted 10 February 2010; published online 12 March 2010)

We report high-performance nanoscale photodetectors utilizing annealed nanocrystal quantum dots (QDs) within a nanoscale metal electrode gap. By optimizing the nanogap size and fabrication process, the device demonstrates a significantly better sensitivity (noise equivalent power = 7.76×10^{-14} W/Hz^{1/2}) and bandwidth (≥ 125 kHz) than previously reported nanoscale photodetectors. Furthermore, by utilizing a lateral photoconduction structure and a self-assembled layer of QDs, the detector fabrication is highly compatible with many substrates and device architectures.

© 2010 American Institute of Physics. [doi:10.1063/1.3356224]

Over the past several years, it has become possible to transmit and manipulate light with exquisite precision on the subwavelength scale through the use of nanostructures.¹ One key component of nearly all optical systems is the photodetector, which translates optical energy into the electrical domain. By combining nanostructures with nanoparticles, subwavelength photodetectors have been demonstrated with high signal-to-noise ratio and the ability to detect low light levels.² Nanoscale photodetectors have the potential to outperform larger, more conventional photodetectors for several reasons. First, the size of a nanoscale detector is intrinsically matched to the size of other nanophotonic components, which decreases energy loss and power consumption without compromising optical coupling efficiency. Second, the spatial confinement inherent in a nanoscale structure leads to a higher density of states and therefore higher quantum efficiencies, while a small device size makes it easier to achieve higher field intensities in the detection region that enhance charge transport. To date, most integrated photodetector structures are based on the PN junction, photoconductor, or metal-semiconductor-metal junction. There has been some research effort to reduce the size of these conventional detectors to the submicron regime, including crossed-nanowire avalanche photodetectors³ and sleeved germanium dipole antenna detectors.⁴ In addition, other device designs have been proposed and demonstrated, including lithographically defined single quantum dot (QD) microwave detectors,⁵ and nanoribbon nanophotodetectors.⁶ In addition to their complex fabrication procedures, each of these devices either have micron-scale active areas, require liquid helium cooling to operate, or have a large overall device footprint. A photodetector with a far-submicron active region operating at room temperature has not yet been demonstrated.

The unique optoelectronic properties of nanocrystal QDs make them an attractive material for photonic devices. Furthermore, the modifiable surface chemistry of colloidal QDs provides a flexible and easy route to fabrication of many devices on a single chip, and the potential to integrate these devices with a variety of nanophotonic components, including waveguides,⁷ nanowires,⁸ and plasmonic structures.⁹ Re-

cently, QDs have been used in large-area photodetectors and solar cells¹⁰ with power conversion efficiencies as high as 4%.¹¹ By building a thin, large-area, vertical photodiode structure on an indium-tin-oxide substrate, the inherently small bandwidth of the QD photodetectors due to tunneling barriers has also been improved to nearly 1 MHz.¹²

Here we report a nanocrystal QD photoconductive photodetector with an active area of approximately 50×60 nm² that can be operated at room temperature in ambient conditions. The structure consists of a thin film of nanocrystal QDs that fill the gap of a lithographically defined metal nanojunction, as shown in Fig. 1(a). Because it relies only upon metal deposition and QD self-assembly, the device can be fabricated on a variety of substrates. Electron transport through the device is limited by the field-induced ionization rate of the photogenerated excitons, which in this case is proportional to the electron-tunneling rate between neighboring nanocrystals. Thus, for high responsivity, it is necessary to have high field intensities across the junction, which can be obtained most easily in a short gap. Figure 1(a) also shows the normal dc electric field in the gap that is, as expected, highly concentrated in and around the nanogap. Furthermore, the short distance between electrodes limits the number of tunneling steps required for electrons to traverse the gap, which also increases responsivity and enhances the speed of the device. By defining the electrode gap with electron-beam lithography (EBL) and annealing the assembled QDs, we observe a significant improvement in sensitivity and bandwidth over both our previously reported devices² as well as recently reported micron-scale QD thin-film photoconductive photodetectors.^{13,14} This improvement is due to the annealing, which reduces the number of trap states and tunneling barriers, the high field intensity in the nanogap which enhances charge transport, and the high absorption cross-section of the active material.¹⁵

The nanogap electrode that consists of a 300 Å Au layer with a 20 Å Cr adhesion layer is patterned by EBL. Figure 1(b) shows a scanning electron micrograph (SEM) of a typical nanogap electrode. The nanocrystals, 620 nm-peak emission CdSe/ZnS core-shell QDs (NN-Labs, LLC) originally suspended in toluene, are precipitated out of solution by ethanol and centrifuged, the supernatant liquid poured off, and the QDs dried in vacuum for 20 min. The QDs are then resuspended in toluene and the process repeated. After the

^{a)}Present address: Intellectual Ventures Laboratory, Bellevue, WA.

^{b)}Author to whom correspondence should be addressed. Electronic mail: lylin@uw.edu.

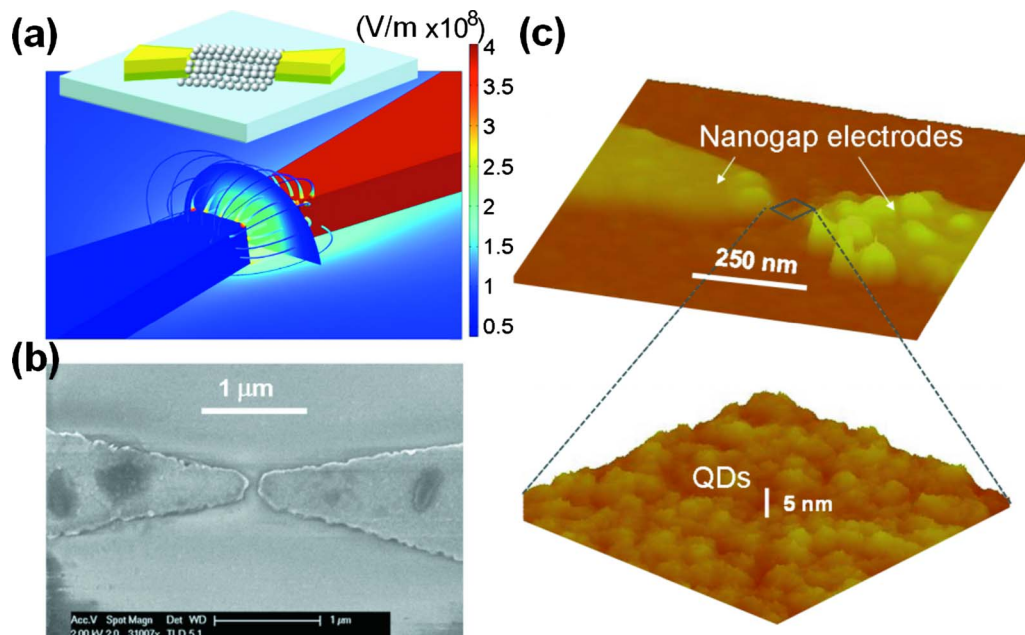


FIG. 1. (Color online) A nanoscale nanocrystal QD photodetector. (a) Illustration of the photodetector device structure and finite element model showing the normal dc electric field concentrated in the gap. Field lines and a cross-section of the field are shown. The unit of the scale bar is $V/cm \times 10^8$. (b) SEM of a typical nanogap electrode without the nanocrystal thin-film. (c) AFM of the device after QD deposition. The zoom-in shows that the QD thin film is quite uniform and smooth, with roughness on the order of the diameter of a single QD.

second washing cycle is complete, the dried QDs are suspended in a 9:1 ratio of hexane/octane and a $5 \mu L$ liquid droplet is micropipetted onto the surface of Au/Cr nanogap electrodes on the glass substrate. After drop-casting of QDs, the film is allowed to dry for 60 s under a fume hood and then, in order to reduce the effect of persistent photoconductivity¹³ and increase the photocurrent through the device, the device is immediately transferred to a pre-heated vacuum chuck for thermal annealing. The sample is annealed at $300 \text{ }^\circ\text{C}$ and 1 mTorr for 40 min, the heat is turned off, and the sample was allowed to cool under vacuum for several hours before device testing. The uniformity of the drop-cast QD film is shown in the atomic force micrograph (AFM) of the device in Fig. 1(c).

For testing the device, different experimental layouts were used depending on the modulation frequency range being measured, as shown in Fig. 2. Light from a 405 nm free-space laser was coupled into an optical fiber and focused onto the photodetector with a spot size of $100 \mu m$. Continuous wave (cw) photocurrent measurements were made with a Keithley 6430 source meter which also served as a dc voltage source. For bandwidth measurements at frequencies below 50 kHz, the laser was electrically modulated and a single SR810 lock-in amplifier was used to measure photocurrent directly, as a function of modulation frequency. The response beyond 50 kHz was measured using the voltage input of a SR844 rf lock-in amplifier with the original 50Ω input impedance terminated with a $1 \text{ k}\Omega$ resistor in order to increase the voltage signal into the amplifier. This reduced the bandwidth of the rf lock-in to approximately 125 kHz. For measurement bandwidths beyond 50 kHz, the noise floor was higher than the actual signal and in order to extract the device response from the noise, the SR844 was used in series with the SR810. The optical input was electrically modulated from 50–200 kHz and also mechanically chopped at 5 Hz. The 5 Hz signal was subsequently detected by the SR810

and the signal time-averaged over many cycles. Data was taken for no illumination as well, and this was used as a baseline for the photocurrent data. Because the single lock-in and double lock-in configurations involved different amplifier gains, the photocurrent was normalized to unity with respect to the baseline data.

Figure 3(a) shows dark and light I-V measurements for a 50 nm nanogap device. The light I-V measurement is made with 14 nW of cw optical power hitting the active area of the photodetector. Here, the photocurrent exceeds the dark current by more than an order of magnitude; the dark current remains below 0.1 pA for a field of $3 \times 10^5 \text{ V/cm}$ while the photocurrent reaches 6 pA under the same field. Figure 3(b) shows the repeatability of a typical device’s performance un-

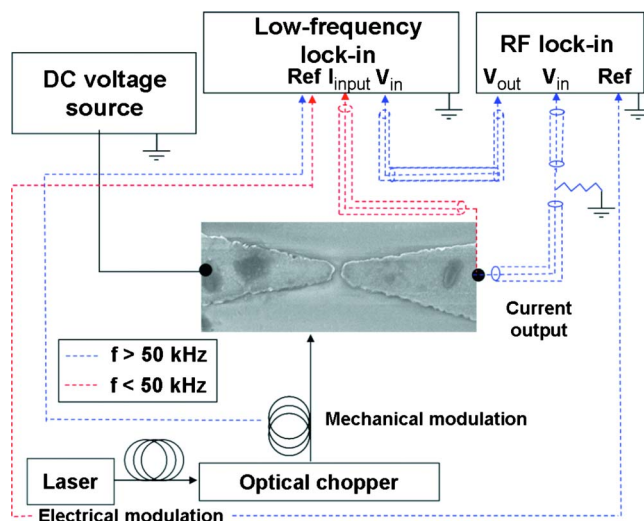


FIG. 2. (Color online) Experimental setup for characterizing sensitivity and bandwidth of the nanoscale QD photodetector. A single lock-in is used for modulation frequency below 50 kHz (red) and a double lock-in approach is utilized for modulation frequency above 50 kHz (blue).

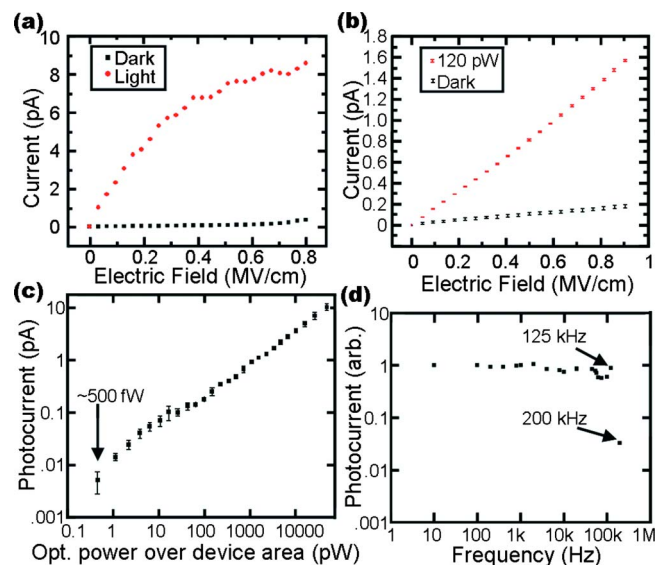


FIG. 3. (Color online) Experimental results for the nanocrystals QD photodetector. (a) Dark (black, square) and light (red, circle) I-V measurement under 14 nW input optical power for a 50 nm nanogap device. (b) Repeatability measurement under low light level illumination (120 pW) for a typical nanogap device. The error bars show the standard deviation associated with five separate data runs for dark and light measurements, respectively. (c) Sensitivity measurement. An input optical power as low as 500 fW can be detected by the 50 nm nanogap QD photodetector. (d) Bandwidth measurement to 200 kHz. The result is limited by the bandwidth of the double lock-in experimental setup (125 kHz).

der lower light level (120 pW) illumination. The error bars show the standard deviation associated with five separate data runs for dark and light measurements, respectively. These measurements were taken in the following order: dark, light, dark, light, etc. Very good repeatability is observed. Figure 3(c) shows photocurrent as a function of optical power hitting the 50 nm nanogap device area. This measurement was performed with a single lock-in amplifier at a light modulation frequency of 1 kHz and an electric field of 8×10^5 V/cm. The standard error is plotted along with the average data from three sets. The lowest measurable optical power was slightly less than 500 fW over the device area of 50×60 nm².

To achieve the high gain and measurement bandwidth necessary to measure the speed of the detector, bandwidth measurements were made in a double lock-in configuration. The results, shown in Fig. 3(d) for the 50 nm nanogap device, indicate that the system response is limited by the instrument bandwidth. There appears to be no 3 dB roll-off at 125 kHz and the instrument itself rolls off beyond this, so it is assumed that the photodetector has a bandwidth of at least 125 kHz. This more than doubles the best reported result for nanocrystal thin-film photodetection devices¹⁶ utilizing simple photoconductor structures.

The absorption coefficient of a typical QD thin-film in the device was characterized to be 18%. Figures of merit were estimated for the 50 nm nanogap device that yielded the result in Fig. 3(c). These calculations are based on a measured photocurrent of 0.1 pA at 17 pW illumination and 8×10^5 V/cm electric field, which results in a responsivity of 5.88 mA/W. The noise current is assumed to be shot-noise

limited and is given by $I_s = (2qIB_n)^{1/2}$, where I is the total current and B_n is the noise bandwidth. Given a dark current of 0.55 pA, as seen in Fig. 3(a), the total current is 0.65 pA, resulting in a noise current spectral density $(I_s^2/B_n)^{1/2}$ of 4.56×10^{-16} A/Hz^{1/2}. The noise-equivalent power (NEP) is given by the noise spectral density divided by the responsivity and is found to be 7.76×10^{-14} W/Hz^{1/2}. The active area of 50×60 nm² in the nanogap was used for the calculation of detectivity. The calculated specific detectivity, $D^* = (A)^{1/2}/\text{NEP}$ where A is the area, is 7.06×10^7 Jones (cm Hz^{1/2} W⁻¹).

In conclusion, we report the design, fabrication, and testing of a nanogap QD photodetector with high sensitivity and bandwidth. The performance of the photodetector is enhanced by the high absorption cross-section of the active material, the high field intensity and small overall tunneling distance in the device. We measure an optical power of 500 fW over the active area of the device and an instrument-limited bandwidth of at least 125 kHz, which outperforms other nanoscale photodetectors reported so far. In addition, the ability to fabricate the photodetector on a variety of substrates provides a unique capability for this technology to be integrated with various photonic and electrical components, and may enable new applications in photonic integrated circuits, telecommunications, or imaging applications.

M. C. Hegg and M. P. Horning thank the NSF IGERT Graduate Fellowship Program and University of Washington UIF Graduate Fellowship Program for financial support. This project was supported in part by the National Science Foundation (Grant No. ECCS-0925378). Work was performed in part at the University of Washington Nanotech User Facility (NTUF), a member of the National Nanotechnology Infrastructure Network (NNIN), which is supported by the National Science Foundation.

¹W. L. Barnes, A. Dereux, and T. W. Ebbesen, *Nature (London)* **424**, 824 (2003).

²M. Hegg and L. Lin, *Opt. Express* **15**, 17163 (2007).

³O. Hayden, R. Agarwal, and C. Lieber, *Nature Mater.* **5**, 352 (2006).

⁴L. Tang, S. Kocabas, S. Latif, A. Okyay, D. Ly-Gagnon, K. Saraswat, and D. Miller, *Nat. Photonics* **2**, 226 (2008).

⁵O. Astafiev, S. Komiyama, T. Kutsuwa, V. Antonov, Y. Kawaguchi, and K. Hirakawa, *Appl. Phys. Lett.* **80**, 4250 (2002).

⁶Y. Jiang, W. Zhang, J. Jie, X. Meng, X. Fan, and S. Lee, *Adv. Funct. Mater.* **17**, 1795 (2007).

⁷L. Huang, M. Hegg, C. Wang, and L. Lin, *Micro & Nano Lett.* **2**, 103 (2007).

⁸M. Law, D. Sirbuly, J. Johnson, J. Goldberger, R. Saykally, and P. Yang, *Science* **305**, 1269 (2004).

⁹J. Dionne, H. Lezec, and H. Atwater, *Nano Lett.* **6**, 1928 (2006).

¹⁰G. Konstantatos, I. Howard, A. Fischer, S. Hoogland, J. Clifford, E. Klem, L. Levina, and E. Sargent, *Nature (London)* **442**, 180 (2006).

¹¹E. H. Sargent, *Nat. Photonics* **3**, 325 (2009).

¹²J. Clifford, G. Konstantatos, K. Johnston, S. Hoogland, L. Levina, and E. Sargent, *Nat. Nanotechnol.* **4**, 40 (2009).

¹³V. Porter, S. Geyer, J. Halpert, M. Kastner, and M. Bawendi, *J. Phys. Chem. C* **112**, 2308 (2008).

¹⁴G. Konstantatos, J. Clifford, L. Levina, and E. Sargent, *Nat. Photonics* **1**, 531 (2007).

¹⁵V. Klimov, *Science* **290**, 314 (2000).

¹⁶D. Oertel, M. Bawendi, A. Arango, and V. Bulovic, *Appl. Phys. Lett.* **87**, 213505 (2005).